Available online at www.sciencedirect.com
SCIENCE DIRECT
Journal of Sound and Vibration 293 (2006) 566–574
JOURNAL OF SOUND AND VIBRATION
www.elsevier.com/locate/jsvi

On the rolling noise generation due to wheel/track parametric excitation

T.X. Wu[a,*], D.J. Thompson[b]

[a]School of Mechanical Engineering, Shanghai Jiao Tong University, Shanghai 200030, PR China
[b]Institute of Sound and Vibration Research, University of Southampton, Southampton SO17 1BJ, UK

Accepted 26 August 2005
Available online 18 January 2006

Abstract

As a discretely supported railway track is essentially periodic, when a wheel rolls over the rail, it experiences the varying dynamic stiffness in a sleeper bay of the track, and thus the wheel and rail is periodically excited at the sleeper-passing frequency. The parametric excitation due to the varying track stiffness, in addition to the roughness or discontinuities on the wheel and rail rolling surfaces, also causes vibration and noise emission. A frequency–time domain methodology is applied for simulation of the wheel/rail interaction due to the parametric excitation. The wheel/rail interaction forces are calculated and Track–Wheel Interaction Noise Software (TWINS) is used to predict the noise radiation due to the parametric excitation at various train speeds. The results are compared with those from a moving irregularity model where no parametric excitation is generated. It is found that the components due to the parametric excitation are not significant at lower speeds compared with those due to the roughness excitation. Use of a moving irregularity model without considering the wheel/track parametric excitation may under-estimate the noise emission level at high speeds.

1. Introduction

Wheel/rail vibration and noise emission can be caused either by roughness or by discontinuities at the wheel and rail rolling surfaces. In addition they can result from a parametric excitation at the sleeper-passing frequency. This is caused by variations in the dynamic stiffness within a sleeper bay of a discretely supported rail track. When a wheel rolls over the rail, it experiences the varying dynamic stiffness in a sleeper bay of the track and thus is periodically excited at the sleeper-passing frequency. As a result, the wheel/rail contact force varies and the track is also excited.

Two main kinds of model have been used to study wheel/rail interactions, a moving irregularity between a stationary wheel and rail, and a wheel rolling on the track. A moving irregularity model in the frequency domain was used by Remington [1] and Thompson [2] for rolling noise prediction. A time domain moving irregularity model was used by Newton and Clark [3] for the wheel/rail impact due to a wheel flat, and also by

*Corresponding author. Tel.: +86 21 6293 2640; fax: +86 21 6283 6359.
E-mail address: txwu@sjtu.edu.cn (T.X. Wu).

0022-460X/$ - see front matter © 2006 Elsevier Ltd. All rights reserved.
doi:10.1016/j.jsv.2005.08.041

Wu and Thompson [4] for the impact noise generation due to wheel flats, where loss of contact occurs between the wheel and rail.

For a discretely supported rail the moving irregularity model cannot deal with the parametric excitation at the sleeper-passing frequency caused by the varying dynamic stiffness in a sleeper bay. The moving wheel model is therefore essential to investigate the effects on wheel/rail interaction due to the parametric excitation.

The response of a discretely supported track to a moving mass/vehicle has been studied by Kisilowski et al. [5], Sibaei [6], Ripke [7] and Nordborg [8]. In Ref. [7] a finite-element model was used to represent the track, and the wheel/rail interaction force was found to vary periodically at the sleeper-passing frequency. In Ref. [8] both time and frequency domain models were used to study a moving wheel/track interaction. The wheel/rail contact force was shown to have a component at the sleeper-passing frequency and its harmonics. Nielsen and Igeland [9] developed a moving wheel/rail interaction model using a method of modal superposition to simplify the track model. Andersson and Dahlberg [10] investigated the wheel/rail impacts at a railway turnout using a finite-element model for the track with a moving vehicle. Dahlberg [11] studied the rail deflection using a nonlinear track model in the time domain during the passage of a high-speed train bogie. Wu and Thompson [12] have developed an equivalent track model with time-varying parameters in the time domain to study wheel/track parametric excitation.

In this work the noise generation of wheel and rail due to the parametric excitation is studied using an equivalent track model in the time domain developed in Ref. [12]. Using this equivalent track model combined with a moving wheel model, the wheel/rail parametric interaction is simulated. The wheel/rail interaction forces are then transformed into the frequency-domain and converted into the form of an equivalent roughness input to a linear model of wheel/rail interaction. Using Track–Wheel Interaction Noise Software (TWINS) the noise emission is predicted due to the parametric excitation at various train speeds. The results are compared with those from a moving irregularity model where no parametric excitation is generated. It is found that the noise components due to the parametric excitation at lower speeds are not significant compared with those due to the roughness excitation. Use of a moving irregularity model may under-estimate the noise emission level at high speeds.

2. Wheel/track interaction model of parametric excitation

Fig. 1 shows the point receptances of a discretely supported UIC 60 rail with the excitation acting at four different positions from above a sleeper to mid-span. They are calculated using a conventional Timoshenko beam model for the rail, which is discretely supported by the rail-pads, sleepers and ballast. The parameters for the rail are: $E = 2.1 \times 10^{11}\,\mathrm{N/m^2}$, $G = 0.77 \times 10^{11}\,\mathrm{N/m^2}$, $\rho = 7850\,\mathrm{kg/m^3}$, $\eta_r = 0.01$, $A = 7.69 \times 10^{-3}\,\mathrm{m^2}$, $I = 30.55 \times 10^{-6}\,\mathrm{m^4}$, $\kappa = 0.4$, where E is the Young's modulus, G is the shear modulus, ρ is the density, η_r is the loss factor of the rail, A is the cross-sectional area, I is the second moment of area and κ is the shear coefficient. The parameters for the discrete support are: $K_p = 350\,\mathrm{MN/m}$, $\eta_p = 0.25$, $K_b = 50\,\mathrm{MN/m}$, $\eta_b = 1.0$, $M_s = 162\,\mathrm{kg}$, $d = 0.6\,\mathrm{m}$, where K_p is the pad stiffness, η_p is the loss factor of the pad, K_b is the ballast stiffness, η_b is the loss factor of the ballast, M_s is the sleeper mass and d is the sleeper span length. These parameters correspond to a track with concrete sleepers and moderately stiff rail pads.

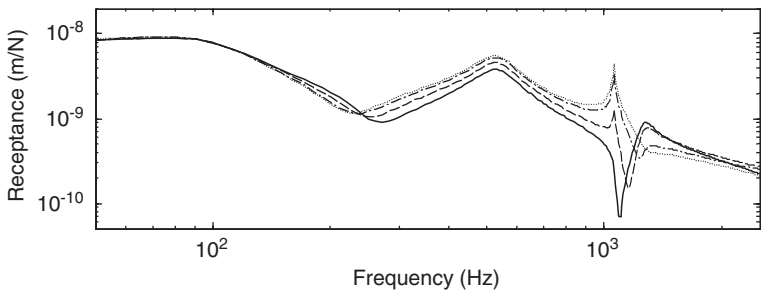

Fig. 1. Receptances of a discretely supported track at different positions, — at a sleeper, ····· mid-span, - - - 0.1 m away from a sleeper, - - - 0.2 m away from a sleeper.

The point receptances for the rail can be seen from Fig. 1 to reach resonance at about 80 and 530 Hz. At 80 Hz the whole track bounces on the ballast stiffness although this resonance is over-damped, while at 530 Hz the rail vibrates on the pad stiffness. The pinned–pinned resonance appears at about 1060 Hz, where the rail receptance reaches a peak at mid-span and a minimum at a sleeper, while at other positions it is mostly between these extremes. The differences in the point receptance between the various positions are mainly around the pinned–pinned resonance frequency and also in the frequency region 250–800 Hz. Fig. 2 shows the variations of the track receptance within a sleeper bay at 350 and 1060 Hz. The receptance at 1060 Hz, where the pinned–pinned resonance occurs, can be observed to vary significantly within a sleeper bay, whereas the receptance variation at 350 Hz is much smaller within a sleeper bay compared with that at the pinned–pinned resonance.

A time-domain model of wheel/rail interaction is used to simulate the wheel/track interaction due to the parametric excitation. Here an equivalent track model from Ref. [12] with time-varying parameters is used. The time-varying model for the track can be set up by firstly using a spatially quasi-static approach in the frequency domain, i.e. working out the receptances of the track at different positions within a sleeper bay under a fixed harmonic force, then transforming the track model in terms of its receptances from the frequency domain into the time domain, and conveying the space-varying dynamic stiffness into the time-varying parameters. This is because the track model is assumed to be linear and thus can be transformed readily from the frequency domain to the time domain. The detailed procedure of this methodology can be found in Ref. [12], and the possible errors caused by using this simplified track model were estimated in Ref. [12]. As the train speed (tens of metres per second) is much lower than the bending wave speed in the beam at audio frequencies (hundreds to thousands of metres per second), the errors caused by using the receptances calculated from a non-moving harmonic force are therefore very limited.

The time-varying track model is mathematically given as

$$(D^n + a_1 D^{n-1} + \cdots + a_{n-1} D + a_n) y(t) = (b_1 D^m + \cdots + b_m D + b_{m+1}) f(t), \tag{1}$$

where D represents the differential operator $\mathrm{d}/\mathrm{d}t$, $y(t)$ and $f(t)$ are the rail displacement at the contact position and the wheel/rail interaction force, respectively, a_i and b_i are the periodically time-varying coefficients due to the varying dynamic stiffness of the track.

This track model can be combined with a moving wheel model to simulate the wheel/rail interaction due to the parametric excitation. The wheel is regarded here as a mass M for simplicity, and the mass is chosen as $M = 600$ kg, including the unsprung mass attached to the wheel. The vehicle is simplified to a static load W acting on the wheel, and it is chosen as $W = 100$ kN. The equation of motion for the wheel mass is in the form

$$M\ddot{x} = W - f, \tag{2}$$

where f is the wheel/rail contact force and is given by

$$f = C_H (x - y - r)^{3/2}, \tag{3a}$$

$$f = 0 \quad \text{when} \quad x - y - r \leqslant 0, \tag{3b}$$

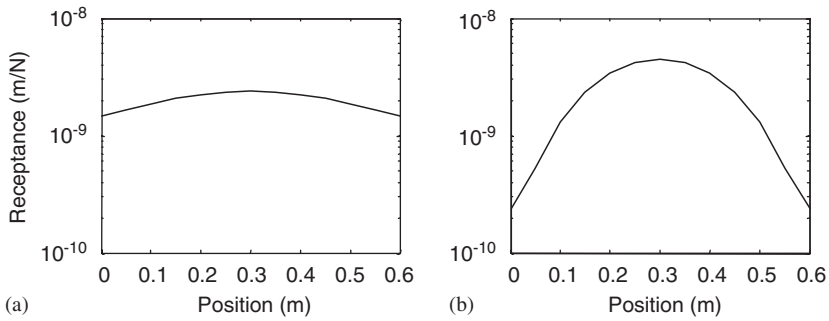

Fig. 2. Magnitude variations of track receptance within a sleeper bay, (a) at 350 Hz, (b) at 1060 Hz.

where x and y are the wheel and rail displacement in the vertical direction at the contact point, respectively, r represents the displacement excitation due to roughness, C_H is the Hertzian constant, taken here as $C_H = 93.7\,\mathrm{GN/m^{3/2}}$. The track and wheel models, Eqs. (1) and (2), are linear, and the track model is time-varying. The wheel/rail interaction model, Eqs. (3a) and (3b), however, is nonlinear. The sign convention adopted here for downward x and y is positive, and for r is positive for a dip, negative for an asperity.

3. Simulations of wheel/track parametric excitation

Simulations of the wheel/track interaction due to the parametric excitation are carried out using Eqs. (1)–(3) and the given parameters. It is assumed first that the wheel/rail interaction and vibration are caused only by the varying dynamic stiffness of the discretely supported track, although in practice, roughness always exists on the wheel and rail contact surfaces.

Fig. 3 shows the results of the wheel/rail interaction due to the parametric excitation of the varying dynamic stiffness of the track. The wheel speed is chosen to be 36 m/s, so that as the distance between sleepers is 0.6 m, the sleeper-passing frequency is 60 Hz. The time 0.1 s in Fig. 3 corresponds to the wheel position above a sleeper. The results are shown in terms of the wheel/rail interaction force in both time series and frequency components. The basic component in the contact force spectrum is shown to be at the sleeper-passing frequency, although high-order harmonics are distributed throughout the frequency range considered. The contact force spectrum also shows a higher level at the pinned–pinned resonance frequency. The reason for this is that the discretely supported track displays a greatest difference in the receptance at the pinned–pinned resonance frequency, refer to Fig. 1. As a result the parametric excitation by the varying dynamic stiffness is

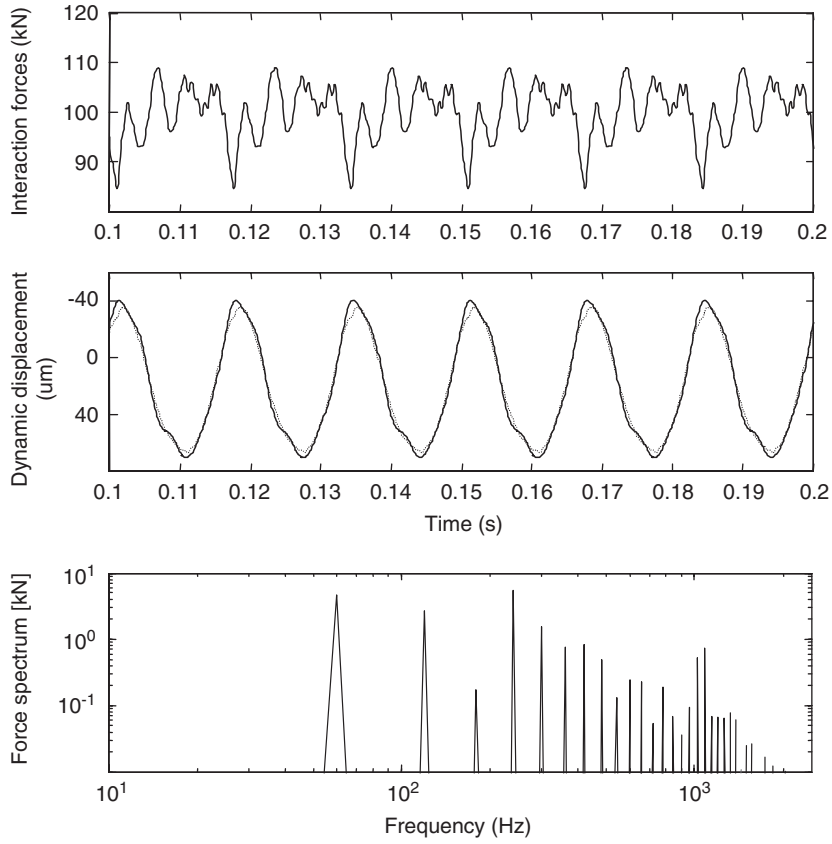

Fig. 3. Wheel/track interaction force and vibration displacement due to the parametric excitation, wheel speed $V = 36\,\mathrm{m/s}$, — rail displacement, ····· wheel displacement.

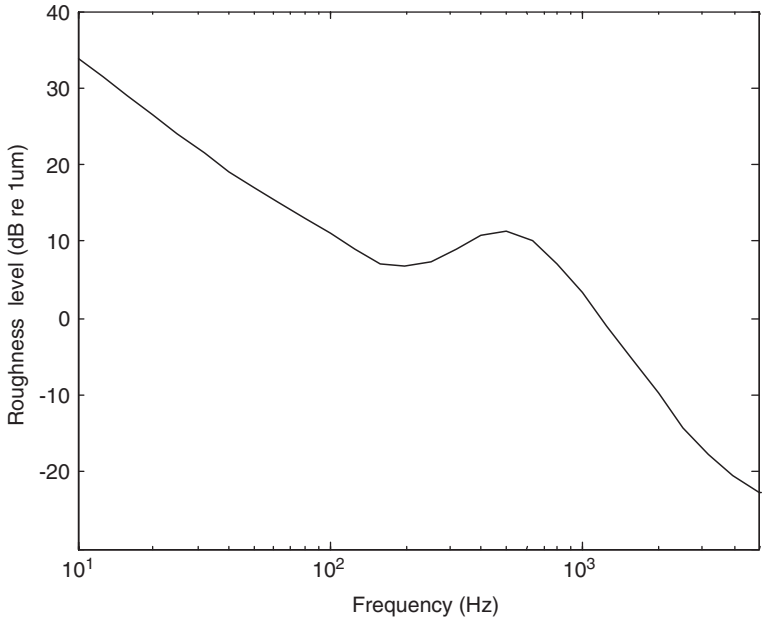

Fig. 4. One-third octave band roughness spectrum of tread-braked wheel on a smooth rail for frequencies corresponding to a train speed of 100 km/h.

larger around the pinned–pinned resonance frequency and thus the variation of the wheel/rail interaction force is higher at these frequencies.

In practice, roughness is present on the rail and wheel contact surfaces. When a wheel rolls on the rail, the roughness forms an excitation with multiple frequency components that can be regarded as a broadband random process. Fig. 4 shows a typical one-third octave band roughness spectrum. This spectrum corresponds to the roughness of a wheel with cast-iron block brakes on a smooth rail [13], and the frequencies correspond to a train speed 100 km/h.

Fig. 5 shows the wheel/track interaction due to the roughness excitation at a train speed 36 m/s (130 km/h), which is transformed from that described in Fig. 4. The results shown are calculated using both the moving wheel and the moving irregularity model for comparison. It can be seen that the wheel/rail contact force from the moving wheel model is a superposition of the forces due to the roughness and parametric excitations. As the roughness input used here is not very severe, some high spikes in the contact force spectra can be clearly seen and they have similar levels to those in Fig. 3 due to the pure parametric excitation without roughness. Apart from these high spikes, the components at other frequencies from the parametric excitation are small because the interaction forces there are mainly caused by the roughness excitation. Moreover, it is observed from Fig. 5 that the wheel/track interaction is dominated by the roughness input, except at 60, 120 and 240 Hz, where the wheel/track interaction shows high peaks due to the parametric excitation.

4. Rolling noise emission due to the parametric excitation

The calculations carried out so far are for the wheel/track interaction force due to the parametric excitation of the varying dynamic stiffness. The rail and wheel are excited by the interaction force and therefore vibrate. The vibration will be transmitted in the form of propagating waves along the rail and within the wheel structure, and thus noise will be radiated.

TWINS models [14], which are linear and operate in the frequency domain using a moving roughness irregularity between a stationary wheel and rail for predicting rolling noise, can be used here to predict the noise radiation due to the parametric excitation. In the TWINS model, considering only the interaction in the vertical direction, the interaction force $F(\omega)$ at angular frequency ω, due to a roughness excitation $R(\omega)$

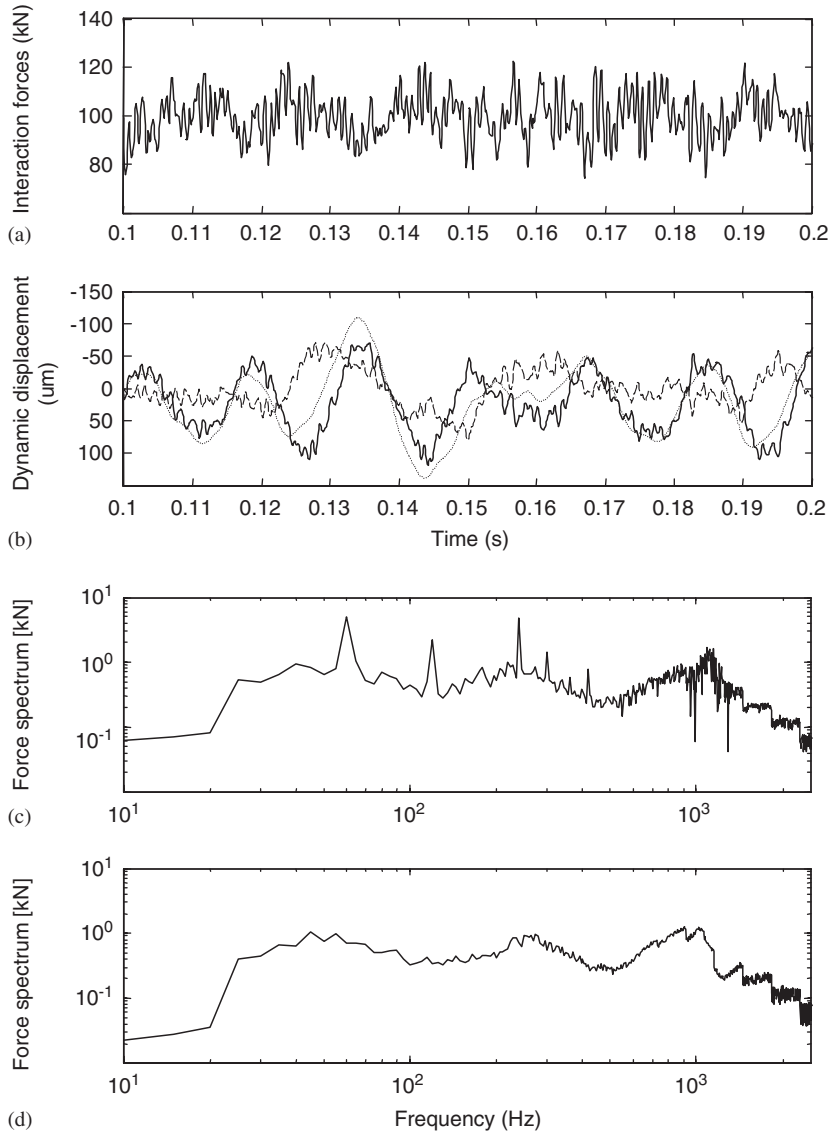

Fig. 5. (a), (b) and (c) wheel/track interaction force and vibration displacement from the moving wheel model (roughness plus parametric excitation), wheel speed $V = 36$ m/s, — rail displacement, ····· wheel displacement, - - - roughness excitation and (d) wheel/track interaction force spectrum from the moving irregularity model.

between the wheel and rail, is calculated by

$$F(\omega) = -\frac{R(\omega)}{\alpha^W(\omega) + \alpha^C(\omega) + \alpha^R(\omega)}, \tag{4}$$

where α^W, α^C and α^R are the receptances of the wheel, contact spring and rail, respectively.

In order to use TWINS to predict noise emission due to the parametric excitation, the interaction force spectrum obtained must be converted back to an 'equivalent roughness spectrum'—the roughness input that would produce the same force spectrum from a linear wheel/rail interaction model used in TWINS. This can be done by using Eq. (4) in reverse

$$R_{\mathrm{eq}}(\omega) = -F(\omega)(\alpha^W(\omega) + \alpha^C(\omega) + \alpha^R(\omega)), \tag{5}$$

where $F(\omega)$ is the wheel/rail interaction force spectrum obtained due to the parametric excitation, α^W is the receptance of the mass wheel and α^R is the track receptance, which is chosen to be the receptance at a sleeper for simplicity, although it varies within a sleeper bay. α^C is the receptance of the contact spring and is from a linear contact spring equivalent to the nonlinear Hertzian contact stiffness. The equivalent roughness spectrum corresponding to the wheel/rail interaction force due to the parametric excitation then can be used as an input into TWINS to predict the noise radiation from the wheel and track [4].

As the difference in the response of the rail vibration to a force between a moving wheel and moving irregularity model is insignificant, only showing two smaller split peaks around the pinned–pinned resonance according to Ref. [7], the noise radiation due to the parametric excitation predicted using TWINS is therefore expected to have only limited errors. In addition, although the interaction force $F(\omega)$ due to the parametric excitation is calculated using the mass wheel model, it has been found in Ref. [4] that the high-frequency modes of the wheel can be taken into account quite precisely by using the equivalent roughness calculated from Eq. (5) as an input to Eq. (4), where the wheel receptance α^W is from a full wheel model, even though these modes are not present in the mass model and thus excluded from the simulations of the wheel/rail interaction in the time domain.

Fig. 6(a) shows the equivalent roughness spectrum in one-third octave band converted from the wheel/rail interaction force due to the pure parametric excitation. Three wheel speeds are chosen, 12, 36 and 60 m/s. The equivalent roughness spectrum can be seen to increase with wheel speed, and the high-level components are at low frequencies. The spectrum also shows higher-level components around the pinned–pinned resonance frequency (1 kHz) in the 60 m/s case. Fig. 6(b) shows the equivalent roughness spectrum due to the roughness plus parametric excitation. It can be observed by comparing Figs. 6(a)–(b) that the equivalent roughness spectrum level due to the pure parametric excitation is generally lower than that due to the roughness input.

Figs. 7(a) and (b) show the total noise power level in one-third octave bands radiated from the wheel and track corresponding to the equivalent roughness spectrum input in Figs. 6(a) and (b), respectively. Compared with the roughness spectrum, the sound power shows higher levels at high frequencies, as the radiation efficiency there is higher than that at low frequencies. The sound power level increases with wheel speed as the roughness spectrum does in Fig. 6. The noise emission due to the parametric excitation can be seen not to be very significant compared with that due to the roughness input.

The rolling noise emissions from the wheel and track at different speeds are shown in Fig. 8 for three cases of the pure parametric excitation, the pure roughness excitation and the roughness plus parametric excitation. For the pure roughness case the wheel/rail interaction is simulated using the moving irregularity model, whereas for the other two cases it is simulated using the moving wheel model. From Fig. 8 the noise emission can be seen to increase with wheel speed in all cases. The noise component from the parametric excitation is limited at speeds up to 48 m/s. Thus the difference in noise emission between the moving irregularity and

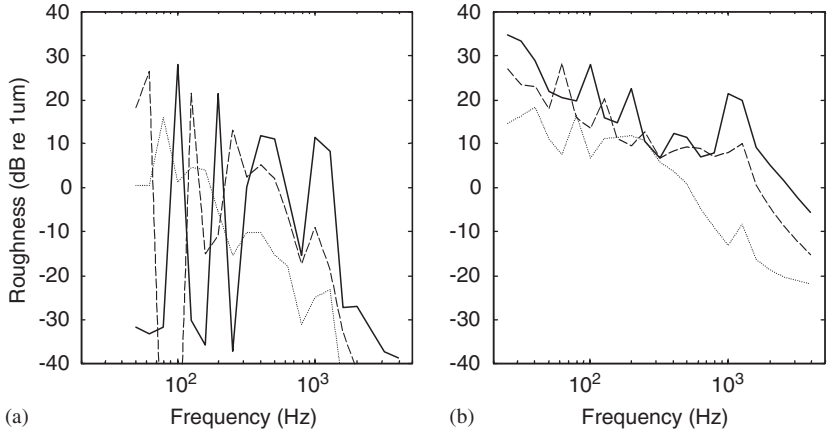

Fig. 6. Equivalent roughness input spectra in one-third octave bands, ····· wheel speed 12 m/s, - - - 36 m/s, — 60 m/s. (a) due to the pure parametric excitation and (b) due to the roughness plus parametric excitation.

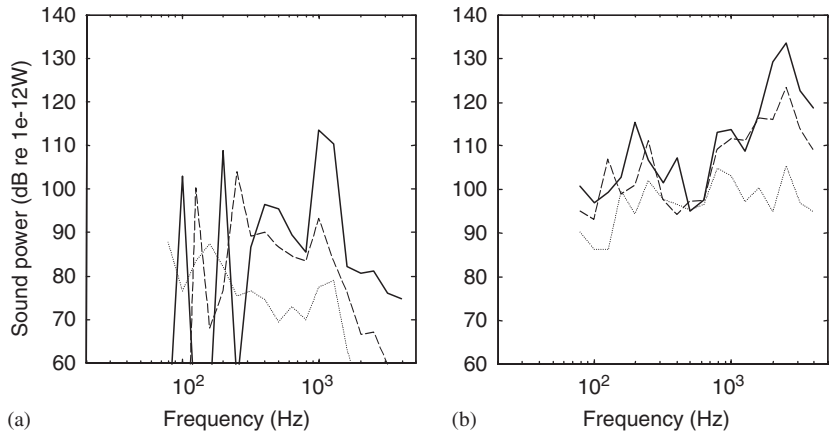

Fig. 7. Sound power level radiated from wheel and track in one-third octave bands, key as for Fig. 6.

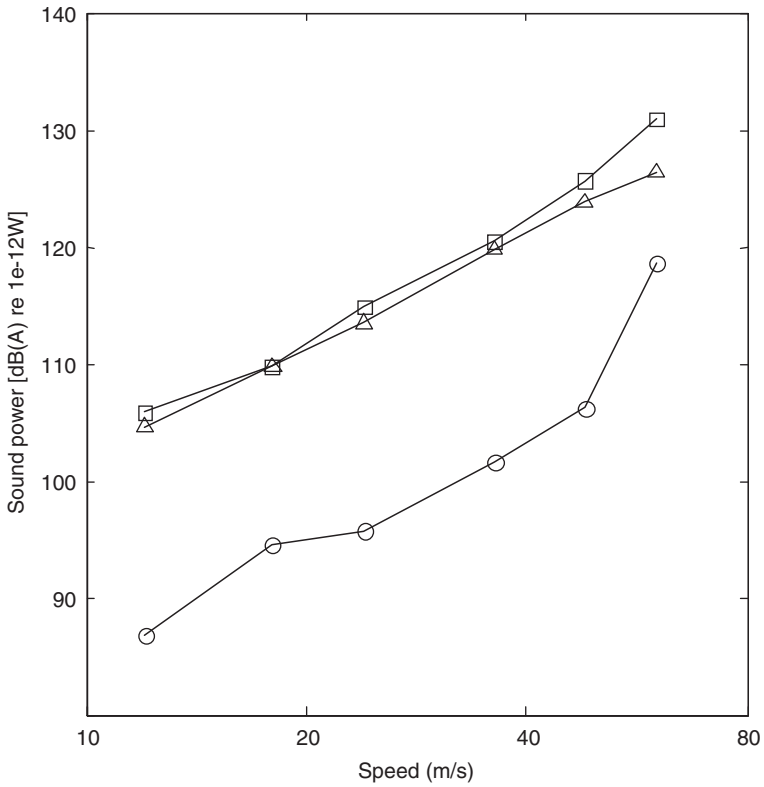

Fig. 8. ○—○ noise emissions due to the pure parametric excitation, △—△ noise emissions due to the pure roughness, □—□ noise emissions due to the roughness plus parametric excitation.

moving wheel model is insignificant at lower speeds. At high speeds, e.g. above 48 m/s, the noise emission from the parametric excitation increases quickly. As a result, the difference in the sound power level between the two models is about 4.5 dB(A) at 60 m/s. Thus use of a moving irregularity model without considering the wheel/track parametric excitation may under-estimate the noise emission level at high speeds.

5. Conclusions

Wheel/track interactions due to the parametric excitation of the varying dynamic stiffness of the discretely supported track are simulated using an equivalent track model combined with a moving wheel model. The wheel/rail interaction force calculated is then converted into the form of an equivalent roughness excitation. Using TWINS models the noise emission is predicted due to the parametric excitation at various train speeds. The results are compared with those from a moving irregularity model where no parametric excitation is generated. It is found that the noise components due to the parametric excitation at lower speeds are not significant compared with those due to the roughness excitation, but use of a moving irregularity model may under-estimate the noise emission level at high speeds.

References

[1] P.J. Remington, Wheel/rail rolling noise I: theoretical analysis, *Journal of the Acoustical Society of America* 81 (1987) 1805–1823.
[2] D.J. Thompson, Wheel–rail noise generation, part I: introduction and interaction model, *Journal of Sound and Vibration* 161 (1993) 387–400.
[3] S.G. Newton, R.A. Clark, An investigation into the dynamic effects on the track of wheelflats on railway vehicles, *Journal of Mechanical Engineering Science* 21 (1979) 287–297.
[4] T.X. Wu, D.J. Thompson, A hybrid model for the noise generation due to railway wheel flats, *Journal of Sound and Vibration* 251 (2002) 115–139.
[5] J. Kisilowski, Z. Strzyzakowski, B. Sowinski, Application of discrete-continuous model system in investigating dynamics of wheel–track system vertical vibration, *Zeitschrift fuer Angewandte Mathematik und Mechunik* 68 (1988) T70–T71.
[6] Z. Sibaei, Vertikale Gleisdynamik beim Abrollen eines Radsatzes—Behandlung im Frequenzbereich, Fortschritt-Berichte VDI, Reihe 11, No. 165, 1992.
[7] B. Ripke, Hochfrequente Gleismodellierung und Simulation der Fahrzeug-Gleis-Dynamik unter Verwendung einer nichtlinearen Kontaktmechanik, Fortschritt-Berichte VDI, Reihe 12, No. 249, 1995.
[8] A. Nordborg, Wheel/rail noise generation due to nonlinear effects and parametric excitation, *Journal of the Acoustical Society of America* 111 (2002) 1772–1781.
[9] J.C.O. Nielson, A. Igeland, Vertical dynamic interaction between train and track—influence of wheel and track imperfections, *Journal of Sound and Vibration* 187 (1995) 825–839.
[10] C. Andersson, T. Dahlberg, Wheel/rail impacts at a railway turnout crossing, *Proceedings of the Institution of Mechanical Engineers, Part F* 212 (1998) 123–134.
[11] T. Dahlberg, Dynamic interaction between train and non-linear railway track model, in: *Proceedings of the Fifth European Conference on Structural Dynamics*, Munich, Germany, 2002.
[12] T.X. Wu, D.J. Thompson, On the parametric excitation of the wheel/track system, *Journal of Sound and Vibration* 278 (2004) 725–747.
[13] P.C. Dings, M.G. Dittrich, Roughness on Dutch railway wheels and rails, *Journal of Sound and Vibration* 193 (1996) 103–112.
[14] D.J. Thompson, M.H.A. Janssens, TWINS: Track–wheel interaction noise software, theoretical manual, Version 2.4, TNO Report TPD-HAG-RPT-93-0214, TNO Institute of Applied Physics, 1997.